Combined Video Analysis of ICG and 5-ALA Induced Protoporphyrin IX and Hemoglobin Oxygen Saturation in near Infrared

T. A. Savelieva[1,2], D. M. Kustov[1], P. V. Grachev[1,2], V. I. Makarov[1], E. E. Osipova[1] and V. B. Loschenov[1,2]

[1]*Prokhorov General Physics Institute of the Russian Academy of Sciences, Vavilov st., Moscow, Russia*
[2]*National Research Nuclear University MEPhI, Kashirskoe sh., Moscow, Russia*

Keywords: Indocyanine Green, Protoporphyrin IX, Haemoglobin Oxygenation, Fluorescence, Diffuse Reflectance.

Abstract: Due to the high recurrence rate after the glial brain tumor removal, methods of intraoperative navigation have a high relevance, providing the most complete removal of tumor tissues with maximum preservation of healthy ones. In this work a combined visualization method is proposed with an assessment of fluorescence and diffuse reflectance images. Fluorescence intensity of 5-ALA-induced protoporphyrin IX allows visualization of tumor cells, distribution of indocyanine green fluorescence helps to visualize the vascular system of the tumor, and parallel mapping of the degree of oxygenation demonstrate the hypoxic regions. The images were obtained in the near infrared range of the optical spectrum in order to maximize the optical probing depth in the window of biological transparency.

1 INTRODUCTION

This paper presents a video analysis technique, which allows parallel-sequential implementation of:
- simultaneous registration of fluorescent intraoperative images of tumors and surrounding tissues in two wavelengths, corresponding to the fluorescence of protoporphyrin IX, which characterizes the activity of metabolic processes in cells, and indocyanine green fluorescence, characterizing the parameters of blood supply to the tissue with the display in the overlay mode of two fluorescent patterns;
- registration of intraoperative images of tumors and surrounding tissues in diffusively reflected light at wavelengths characterizing the ratio of oxy- and deoxyhemoglobin to assess the degree of hypoxia of different sections of tumor tissue.

Currently there are no systems for simultaneous visualization of fluorescence of indocyanine green and protoporphyrin IX in clinical practice, however, these modes are available sequentially in the Zeiss Opmi Pentero microscope, but there are no oxygen saturation mapping regime. The possibility of a multi-factorial intraoperative assessment of the tumor state can improve the accuracy of resection. There are a number of works on simultaneous registration of the photosensitizer fluorescence distribution and the image of the same area in diffusively reflected broadband light to observe the fluorescent tissues on the full color background image and thereby improve navigation (Sato et al., 2015; Loshchenov et al., 2018). In other side the hemoglobin oxygenation visualization of brain tissues by optical methods are performed in two ways as a rule. Oximetric video systems in the visible or near infrared spectral range are based on mathematical processing of full-color images (Mustari et al., 2018) or hyperspectral imaging (Giannoni et al., 2018). But using the near infrared region for this purpose is limited as a rule by the mapping of spectroscopic signals obtained from specific points of the cortex projection from a set of fiber optic probes, as in Hitachi, fNIR Devices LLC, Biopac, Artinis systems for functional near infrared spectroscopy. These systems are designed for functional transcranial spectroscopy in the near infrared, while proposed system is intended for intraoperative imaging of the tumor bed. And it has such an important advantage over visualization systems in the visible range as work in the biological transparency window. As it is well known, in near

Savelieva, T., Kustov, D., Grachev, P., Makarov, V., Osipova, E. and Loschenov, V.
Combined Video Analysis of ICG and 5-ALA Induced Protoporphyrin IX and Hemoglobin Oxygen Saturation in near Infrared.
DOI: 10.5220/0007693703200324
In *Proceedings of the 7th International Conference on Photonics, Optics and Laser Technology (PHOTOPTICS 2019)*, pages 320-324
ISBN: 978-989-758-364-3

infrared range of optical spectrum the absorption of main tissue chromophores is minimal so the light can penetrate deeper in the tissue. But in this optical range we should consider the prevalence of scattering under the absorption in tissue.

2 MATERIALS AND METHODS

2.1 Device

The four laser light sources were used. The source with 635 nm wavelength was used for PpIX fluorescence excitation. The source with 785 nm wavelength was used for ICG fluorescence excitation. The 687 nm laser light source was used for getting diffuse reflectance image in the position where deoxygenated hemoglobin absorption significantly higher than oxygenated hemoglobin absorption. The source with 805 nm wavelength was used to obtain diffuse reflectance image in the position close to isosbestic point of deoxygenated and oxygenated hemoglobin absorption spectra. Two video cameras were used for parallel-serial data reception in two modes: fluorescence and diffuse reflectance image registration.

In fluorescence mode in front of the cameras were installed such optical band-pass filters as 710/40 Semrock for Pp IX fluorescence registration and 832/37 Semrock for ICG fluorescence registration.

In diffuse reflectance mode in front of the cameras were installed 685/40 Semrock and 810/10 Semrock band-pass filters to eliminate cross light from these spectrum ranges.

The control of oxygenation level was performed with fiber-optic spectroscopy technique with LESA-01-BIOSPEC using algorithm described earlier (Stratonnikov et al., 2006). The control of fluorescence intensity was carried out with the same spectroscopic device in fluorescence mode.

2.2 Diffuse Reflectance Image Processing Algorithm

Schmitt and Kumar, (Schmitt and Kumar, 1996; Kumar and Schmitt, 1997), demonstrated the dependence of the diffuse reflectance spectrum in the near infrared region for tissue with different optical properties on the distance between the illuminating and receiving fibers, using the diffusion approximation to approximate the obtained dependences. For the fluorescence spectra, it is usual to assume that measuring the diffuse reflectance spectrum of tissues in the same range as fluorescence one is sufficient to take into account the effect of the sample geometry. However, as it was shown in Gebhart et al., 2007, the spectra of diffuse reflectance and fluorescence show significant differences when registering by the method of point to point spectroscopy in contact with the sample and at a certain distance, as well as by the method of spectrally resolved visualization. An increase in the contrast between the red and blue-green ranges of the diffuse reflectance spectrum was found for the illumination-reception geometry implemented in the visualization system and point spectroscopy at a certain distance from the sample. This effect is most likely due to the low contribution of multiply scattered photons in case of proximity of light source and receiver. Differences in the diffuse reflectance spectrum from samples containing hemoglobin in various concentrations were greater for the imaging system compared to the point spectroscopy system, but they had similar trends. At the same time, the dependence of the diffuse reflectance spectra of samples with different contents of scatterers differed for the considered geometries both in nature and in magnitude. In this connection, in the present work, in order to consider the influence of the measurement geometry, a mathematical simulation was carried out for the cases of the diffusely reflected and fluorescent radiation registration at different distances between the illumination and receiving fibers for different numerical apertures.

2.3 Objects for Validation

Validation of proposed method of combined video analysis and image processing algorithms was carried out on an array of optical phantoms that simulate the optical properties of nerve tissues containing the studied photosensitizers with a concentration 0.625 mg/l, 1.25 mg/l, 2.5 mg/l and 5 mg/l of indocyanine green and 1.25 mg/l , 2.5 mg/l, 5 mg/l and 10 mg/l of Pp IX. Photosensitizers were diluted with the 1% fat emulsion solution as a scattering agent to simulate multiple scattering occurring in investigated tissues.

Phantoms were performed in the cuvettes. To analyze their images in environments similar to the natural brain, they were immersed in a scattering gelatin matrix (5% gelatin with a 1% intralipid solution).

Optical phantoms simulating biological tissue with blood were also performed. Whole blood was diluted 16 times so that the hemoglobin concentration was approximately equal to the

average concentration in the white matter of the brain. Fat emulsion solution was used as a scattering medium. The samples were deoxygenated through nitrogen ventilation.

Testing of the developed method and system on laboratory animals was also carried out in the fluorescence mode (with simultaneous administration of indocyanine green and protoporphyrin IX) and in the diffuse reflectance mode (to control the degree of oxygenation) before, during and after deoxygenation of the animal's blood by nitrogen ventilation.

3 RESULTS AND DISCUSSION

3.1 Analysis of Co-distribution of ICG and PP IX on Optical Phantoms

The results of the video system validation on optical phantoms are shown in Figure 1 in the fluorescence mode for fluorescence phantoms. In the left column of images in black-white channel the laser light source with 785nm wavelength for fluorescence excitation and optical filter 832/37 nm for fluorescence registration were used. In the right column of images in color channel the laser light source with 633 nm wavelength for fluorescence excitation and optical filter 710/40 nm for fluorescence registration were used. These two pictures can be combined in one in special mode to navigate during surgery.

Validation showed that the sensitivity of the system in the fluorescence mode is no worse than 1.25 mg/l for indocyanine green detection and 0.125 mg/l for Pp IX detection without hardware signal amplification in real time for fluorescent inclusions in the scattering medium, whose transverse dimensions do not exceed 1 mm.

3.2 Algorithm of Diffuse Reflectance Image Processing with Separation of Absorption and Scattering Component

The diffuse reflectance spectra depends on scattering as well as absorption of light by the tissue. If the purpose of registering a diffuse reflectance signal is to analyze the content of chromophores in a tissue by their absorption, these two processes should be separated. At the same time, information about tissue scattering can be an independent diagnostic criterion.

In a highly scattering medium, the radiation corresponding to one pixel of the image is characterized by a wide distribution of photon path lengths in the tissue. Thus, the greater the scattering compared to the absorption, the greater the influence of the neighboring pixels on each other. In general case, the solution for one pixel of the image is a linear combination of solutions for a point source and a receiver for the sum of possible photon paths in the tissue.

As a result of numerical simulation of the propagation of light in a high-scattering medium with optical properties, which varied in a series of physiologically relevant values, the following approximating dependence of the diffuse reflection signal (Rd) on absorption coefficient (μ_a) and scattering coefficient (μ'_s) was proposed:

$$R_d(\mu_a, \mu'_s, x) = A_1 \cdot \mu'_s \cdot e^{-(B_0 + B_1 \cdot \mu'_s + B_2 \cdot \mu_a)} \quad (1)$$

Here, A_1 and B_i are adjustable parameters which depend on the illumination and signal detection geometry, μ'S, reduced scattering coefficient defined as $\mu'_s = \mu_s \cdot (1 - g)$, g, scattering anisotropy factor, and μa, absorption coefficient. Detailed description of this approximation is given in earlier publication (Savelieva et al., 2015).

R_d is the signal that we receive from each camera (on two wavelengths) in the diffuse reflection mode of registration, taking into account the normalization to the image of standard white illuminated with the same broadband light source. Solving equation (1) we get the values of the absorption coefficients on chosen wavelengths.

The matrix for converting the concentrations of tissue chromophores studied in this work to absorption coefficients is as follows:

$$\begin{bmatrix} \mu_a^{\lambda 1} \\ \mu_a^{\lambda 2} \end{bmatrix} = \ln(10) \cdot \begin{bmatrix} \varepsilon_{Hb}^{\lambda 1} & \varepsilon_{HbO2}^{\lambda 1} \\ \varepsilon_{Hb}^{\lambda 2} & \varepsilon_{HbO2}^{\lambda 2} \end{bmatrix} \cdot \begin{bmatrix} c_{Hb} \\ c_{HbO2} \end{bmatrix} \quad (2)$$

where $\mu_a^{\lambda i}$ – absorption coefficient on wavelength λ_i, $\varepsilon_j^{\lambda i}$ – molar extinction coefficient of j chromophore on wavelength λ_i, C_j – the concentration of j chromophore.

Solving system of equations (2) we get the values of deoxygenated hemoglobin concentration (c_{Hb}) and oxygenated haemoglobin concentration (c_{HbO2}). From these parameters we can calculate the deoxygenation parameter as:

$$Deox = c_{Hb}/(c_{Hb} + c_{HbO2}) \quad (3)$$

This parameter was introduced in this work for more convenient observation and it is additional to

the level of hemoglobin oxygen saturation; in total, they give 1.

On Figure 2 we can see two pictures in diffuse reflectance mode as an example of registered images.

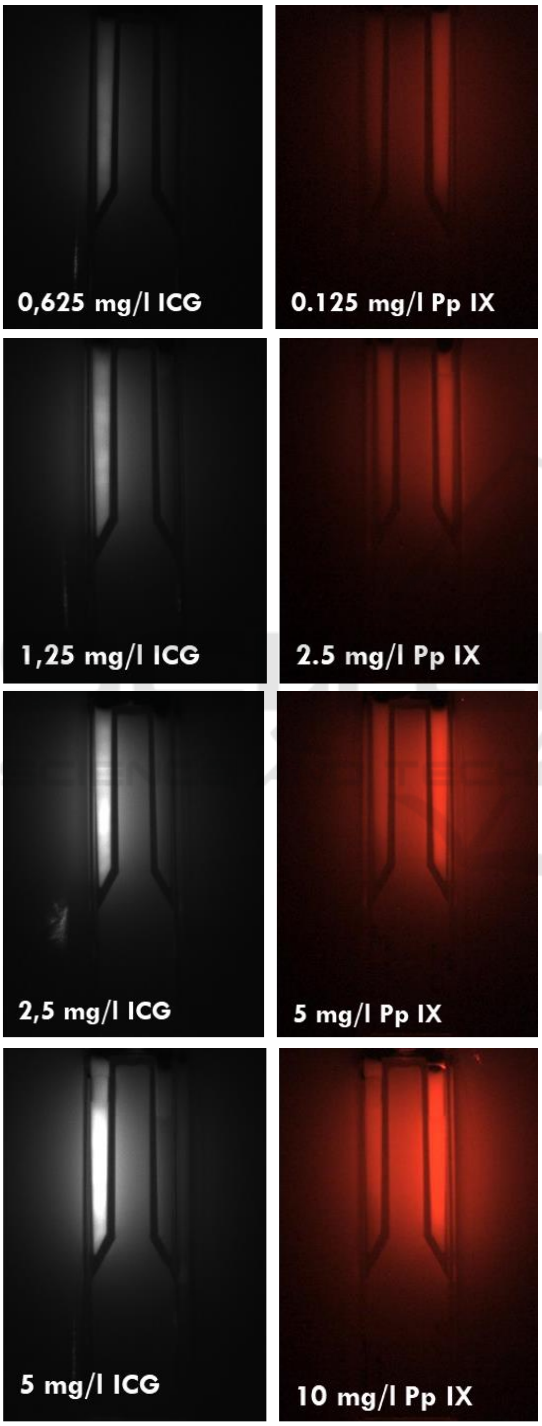

Figure 1: Imaging of distribution of ICG and Pp IX in optical phantoms in fluorescence mode.

3.3 Analysis of Hemoglobin Oxygen Saturation with Diffuse Reflectance Visualization in NIR Region

The time dependences of the deoxygenation parameter (the ratio of the deoxygenated hemoglobin concentration to the total concentration of hemoglobin) were obtained during nitrogen ventilation of an optical phantom containing a solution of whole blood in the scattering medium, which served as calibration curves for analyzing similar dependencies recorded in experiments with laboratory animals. On Figure 2 we can see the example of pictures in two wavelengths obtained during *in vivo* experiment. Laboratory animals were ventilated with nitrogen to achieve significant changes in the deoxygenation parameter without harming the animal's health.

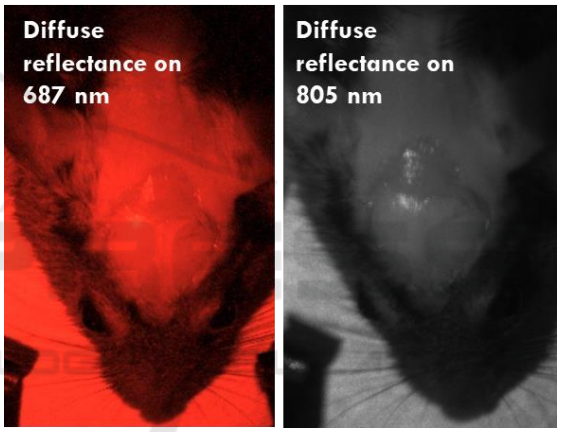

Figure 2: Imaging of optical scattering phantoms with haemoglobin in diffuse reflectance mode.

The curve of change in the deoxygenation parameter of the animal brain depending on the ventilation time is shown in Figure 3.

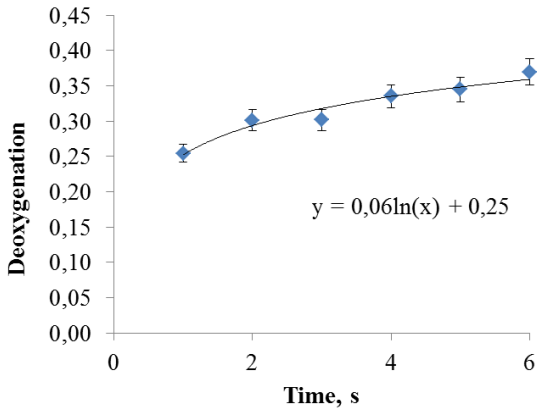

Figure 3: Analysis of deoxygenation in NIR *in vivo*.

4 CONCLUSIONS

The video analysis technique for intraoperative navigation during neurosurgery is proposed that allows simultaneous registration of fluorescent intraoperative images of tumors and surrounding tissues at two wavelengths corresponding to the fluorescence of protoporphyrin IX, which characterizes the activity of metabolic processes in cells, and fluorescence of indocyanine green, which characterizes the parameters of tissue blood supply with display in mode overlaying two fluorescent pictures, as well as recording of intraoperative images of tumors in diffusevely reflected broadband light to measure the degree of tissue hypoxia.

ACKNOWLEDGEMENTS

The reported study was funded by RFBR according to the research project № 17-00-00162 (K) (17-00-00159) and partially supported by the Competitiveness Program of MEPhI.

REFERENCES

Sato, T., Suzuki, K., Sakuma, J., Takatsu, N., Kojima, Y., Sugano, T., Saito, K., 2015, *Development of a new high-resolution intraoperative imaging system (dual-image videoangiography, DIVA) to simultaneously visualize light and near-infrared fluorescence images of indocyanine green angiography. ActaNeurochirurgica*, Volume 157, Issue 8, pp 1295–1301.

Loshchenov, M., Blondel, W., Amouroux, M., Steiner, R., Potapov, A., Golbin, D., Loran, O., Babaev, A., Borodkin, A., Daul, C., Trinh, D.-H., Loschenov, V., 2018, *Multimodal fluorescence imaging navigation for surgical guidance of malignant tumors in photosensitized tissues of neural system and other organs*, Proc. SPIE 10677, Unconventional Optical Imaging, 106773N.

Mustari, A., Nakamura, N., Kawauchi, S., Sato, S., Sato, M., Nishidate, I., 2018, *RGB camera-based imaging of cerebral tissue oxygen saturation, hemoglobin concentration, and hemodynamic spontaneous low-frequency oscillations in rat brain following induction of cortical spreading depression*, Biomed. Opt. Express 9, 933-951.

Giannoni, L., Lange, F., Tachtsidis I., 2018, *Hyperspectral imaging solutions for brain tissue metabolic and hemodynamic monitoring: past, current and future developments*. J. Opt. 20 044009

Stratonnikov, A.A., Meerovich, G.A., Ryabova, A.V., Savel'eva, T.A., Loshchenov, V.B., , 2006, *Application of backward diffuse reflection spectroscopy for monitoring the state of tissues in photodynamic therapy*, Quantum Electronics, vol. 36, no. 12, pp. 1103–1110.

Schmitt, J. M., and Kumar, G., 1996, *Spectral distortions in near-infrared spectroscopy of turbid materials.* //Appl. Spectrosc. 50, 1066–1073.

Kumar, G., Schmitt, J. M., 1997, *Optimal probe geometry for near-infrared spectroscopy of biological tissue*. //Appl. Opt., 36, 2286–2293.

Gebhart, S. C., Majumder, S. K., Mahadevan-Jansen, A., 2007, *Comparison of spectral variation from spectroscopy to spectral imaging.* //Applied Optics, 46(8).

Savelieva, T. A., Loshchenov, V. B., Goryainov, S. A., Shishkina, L. V., and Potapov. A. A., 2015, *A spectroscopic method for simultaneous determination of protoporphyrin IX and hemoglobin in the nerve tissues at intraoperative diagnosis, Russian Journal of General Chemistry*, vol. 85, no. 6, pp. 1549–1557.